RECENT TRENDS IN CHEMICAL SENSOR TECHNOLOGY

Abstract

Recently, the interest in development of rapid, sensitive and selective smart gas sensors devices has increased for environment protection and healthcare uses. Substantial exploration has been carried out in the field of sensor technology. Nevertheless, there exist certain challenges. This chapter discusses the fundamentals of chemical gas sensors, sensor characteristics, gas sensing performance-enhancing methods, Factors influencing the performance of gas sensor, Ways to improve the sensor performance, Sensing mechanism, Types of adsorption depletion models.

Authors

F. I. Shaikh
Department of Forensic Physics
Government Institute of Forensic Science
Nipatniranjan Nagar, Aurangabad-431004 (M.S.), India
faiyyajshaikhb4u@gmail.com

R. M. Borade
Department of Forensic Chemistry
Government Institute of Forensic Science
Nipatniranjan Nagar, Aurangabad-431004 (M.S.) India

S. S. Suryavanshi
Punyashlok Ahilyadevi Holkar Solapur University Dnyanteerth Nagar, Kegaon
Solapur-Pune National Highway, Solapur-413255, Maharashtra (India)

I. INTRODUCTION

A sensor is a device which can sense and respond to a stimulus. The stimulus can be the physical or chemical property. The sensor purpose is to sense to some form of an input and convert it into electrical signal. Sensor responds to a physical or chemical impetus then transfers an appropriate output signal [1, 2]. In general, sensor converts nonelectrical quantities into electrical signals.

Currently, the rise in environmental pollution and industrializations sensors has involved vast concern in the field of environmental safety for monitoring and control of toxic gas emission. Therefore, there is an urgent need to develop the gas sensors. The gas sensors have several applications in the field of industrial manufacturing, health care, defence, mines, agriculture, quality control, weather forecast departments etc. [3-7].

The gases to be detected and monitored can be classified into three broad categories :

1. **Oxygen:** It is involved in the monitoring of atmospheric oxygen in boilers and internal combustion engines. These processes require 20% and 5% oxygen concentration respectively.
2. **Toxic gases:** In case of occupational health safety at different workstations the toxic gases must be detected and measured. The range of exposure limit for toxic gases from 1 to several hundred ppm.
3. **Flammable gases:** Most of the flammable gases have the lower explosive level (LEL) up to a few percent.

The gas sensors are also broadly categorized on the basis of technology as follows: Solid State, Spectroscopic and Optic gas sensors. Spectroscopic gas sensors work on the basis of the analysis of the molecular mass or vibrational spectrum of the various test gases. The sensors can be employed for precise quantification of the test gas concentration. Optical sensors are based on the target gas absorption spectra. These sensors require a complex set up comprising a monochromatic source and detector for the absorption spectra analysis of the various test gases.

However, the optic and spectroscopic gas sensors are not only costly but also difficult to implement in reduced space. Whereas, Solid State gas sensors have several benefits such as cost effective, fast response, simple execution and portable [9-11]. The principle of the solid state gas sensor is change in physical and/or chemical properties of the sensor in the presence of the test gases. Amongst the several solid state gas sensors, the metal oxide semiconductor sensors based on SnO_2 [12, 13], In_2O_3 [14], Fe_2O_3 [15], ZnO [16], WO_3 [17], TiO_2 [19] and $LaFeO_3$ [18] etc. are being extensively studied. The transition metal oxides like SnO_2, TiO_2, ZnO etc. seem to be the most suitable materials to be used as gas sensors. The working principle of these gas sensors is the change in the resistance upon the exposure of various test gases. However, these materials exhibits some problems such as cross selectivity and higher operating temperatures. For improving the sensing performance of these gas sensors normally two methods are employed; one of the extensively used method is addition of several metals/metal oxides such as Zn [20], Ni [21], Co [22], Ce [23], Cu [24], Sm_2O_3 [25] etc. whereas in the the second method the sensing material is loaded with the noble metals, (Pd, Pt, Ru, and Au) to promote electronic sensitization.

Metal oxides at higher temperature exhibit change in resistance depending on the target gas composition. Metal oxide semiconductors are known to be of either p-type or n-type semiconductors. For n-type metal oxide semiconductors, the resistance decreases with the concentration of reducing gases, on the other hand it increases with oxidizing gas. The converse is true for p-type semiconductors. The structural and morphological properties such as particle size, surface-to-volume ratio, pore volume and pore size etc. strongly affects the gas sensor performance. In addition to this it is reported that the sensor response properties are also influenced by the synthesis method

1. **Fundamentals of MOX gas sensor:** MOX gas sensors when heated to a suitable temperature in the presence of air respond to various oxidizing and reducing analyte gases through gas sensing mechanism as follows:

   - **Diffusion of gases**
   - **Adsorption of gases**
   - **Surface reaction**
   - **Desorption of reaction products**
   - **Diffusion of reaction products.**

   The diffusion of gases to active region is governed by the surrounding atmospheric temperature. When test gas molecules diffuse into the active layer, these have a tendency to adhere to the sensor surface via. adsorption. The process of adsorption can take place through two different ways namely Physisorption and Chemisorption. In physisorption, the gas molecules are adhered to a sensor surface by weak forces such as van der Waals force. In chemisorption, the gas molecules are attached to the sensor surface by the process of re-arrangement of the electron density. At the sensor surface, the atoms are partly coordinated having unsatisfied dangling bonds [27]. In case of an ionic crystal like SnO_2 both cations and anions have poor coordination. The surface cations are having an incomplete shell of negative oxide ions. Following mechanism explains the sensor behaviour in the measurand environment [28].

   $$\frac{1}{2}O_2 + e^- \leftrightarrow O^-_{ads} \quad \text{------ (1.1)}$$

   $$R_{gas} + O^-_{ads} \rightarrow RO_{gas} + e^- \quad \text{------ (1.2)}$$

   Oxygen gets adsorbed by extracting an electron from the conduction band and dissociates to form various species such as O^-, O^{2-} and O_2^-. This leads to the depletion region formation near the sensor surface. Figure 1.1 and 1.2 depicts the 2D view of the crystallite of sensing material on oxygen adsorption and the band bending respectively. It can be ascribed to the formation of charged double layer at the sensor surface.

Figure 1: 2-D view of the depletion region in presence of atmospheric oxygen.

Figure 2: Corresponding energy band diagram.

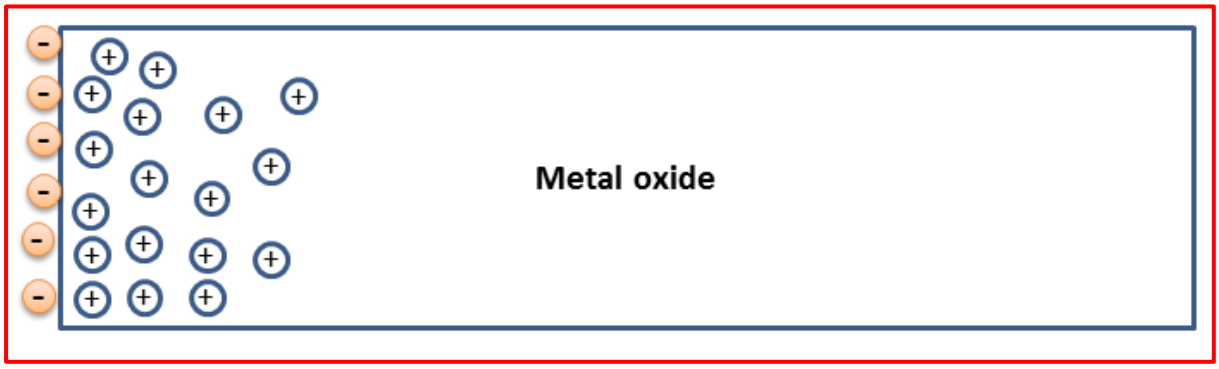

Figure: 3 Distribution of charges for metal-oxide semiconductor (n-type) surface on oxygen chemisorption.

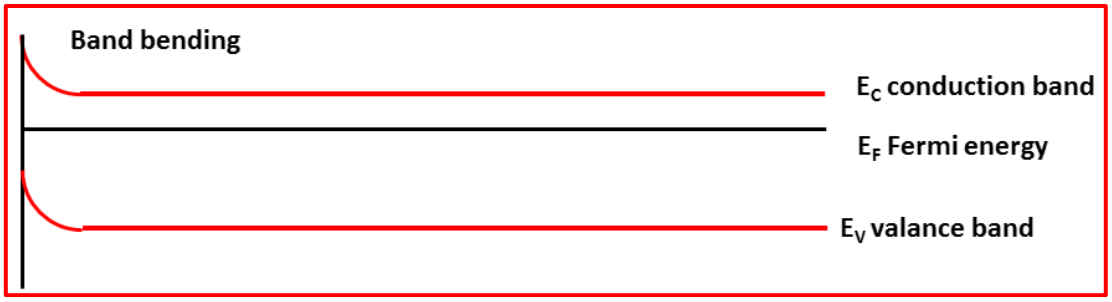

Figure 4: Energy band diagram of MOX (n-type) on oxygen chemisorption.

When the reducing gas is exposed to sensor, it reacts with the O^- adsorbed species forming H_2O molecule. Hence the electron is released back to the conduction band. This decreases the resistance of the semiconducting material. The competition between oxygen removing the electrons and the reducing gases releasing the electrons back is established [27]. Since the atmospheric concentration of oxygen is constant, the resistance depends on the concentration of reducing gas. The competing reactions are shown by equation (1.3) and (1.4) as below:

$$\frac{1}{2}O_2 + e^- \leftrightarrow O^-_{ads} \quad \text{--------- (1.3)}$$

$$H_2 + O^-_{ads} \rightarrow H_2O + e^- \quad \text{\_\_\_\_\_(1.4)}$$

When the reducing gas concentration in this case H_2 concentration rises, the O^- species concentration decreases. This results in increase in the concentration of electron in the conduction band. Hence, the resistance of the sensor is decreased. There is another model that may exist or coexists along with this. If the reducing gas is chemically active, it extracts lattice oxygen from the metal oxide resulting in the generation of vacancies. These oxygen vacancies can act as donors. The atmospheric oxygen oxidize the donor vacancies again. Consequently there is a competition between the oxygen removing donor vacancies and the reducing gas creating donor vacancies at the surface. The number of donor vacancies are governed only by the concentration of reducing gas as oxygen pressure is constant. This is depicted by equation (1.5) as below [27]:

$$CO + M^{2+} + O_L^{2-} \rightarrow CO_2 + M^{2+} + 2e^- \quad \text{---------- (1.5)}$$

Where M is the metal cation and OL is the lattice oxygen. Consequently there separate sensing mechanism for reducing and oxidizing analyte gases respectively. In the first mechanism there is a change in resistance on account of the extraction and release of electrons on account of the surface reaction between the reducing gas and adsorbed oxygen species. In second mechanism there is a creation of donor vacancies on account of the removal of lattice oxygen by combustible gas. The donor vacancies inject charge carriers into the conduction band of the semiconductor. As a result of this there is a change in electrical resistance of the sensor. The chemosorbed gas species continue to remain adsorbed forever or reacts with the sensor causing sensor poisoning or desorb and diffuse back into the surrounding. After desorption and diffusion of gas, the sensor becomes ready for the next measurement.

2. **Classification of sensor:** Sensors are generally categorized depending upon their principle of conversion (the physical or chemical effects on the basis of which they operate) as physical sensors and chemical sensors (Figure 1.5) [29]. Physical sensors are based on physical properties like ionization, magnetostriction, piezoelectricity, photoelectric effect, magnetoelectric effect, and thermoelectric effect etc.

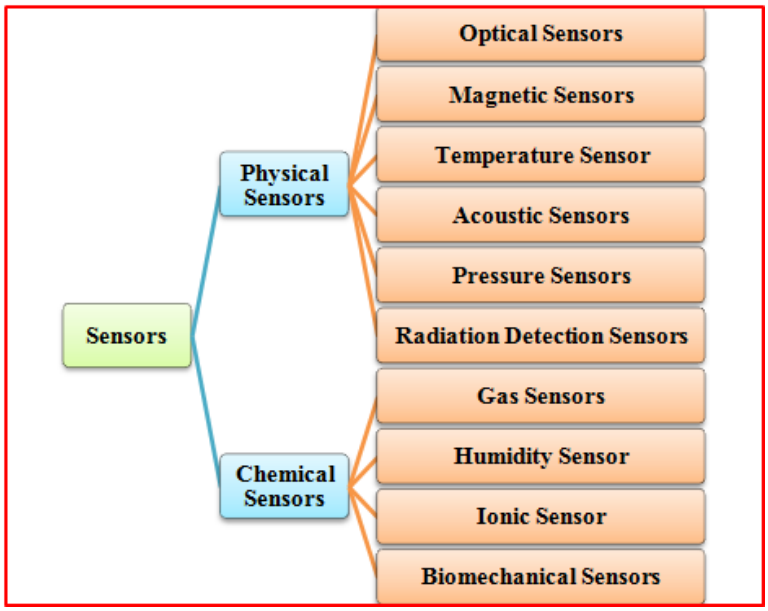

Figure 5: classification of sensor

3. **Chemical sensor:** Chemical sensor transforms chemical information such as concentration into an analytical useful signal [30]. These devices are miniature as a portable devices designed for the selective and continuous on-line monitoring of specific gas concentration in the complex samples. The basic components of the chemical gas sensors are as follows:

   - Sensing element
   - Chemical/analyte/gas recognition system
   - The physicochemical transducer.

4. **Classification of chemical gas sensors:** The chemical sensors there is a change in some physical properties such as mass, volume, resistance etc. The corresponding changes in the physical entity are perceived by the sensor, and directly converted in to some electrical signal by transducer. Depending on the types of chemical reactions and the signal transformation there are several types of sensors. These are amperometric [31], volumetric [32], conductometric [33], potentiometric [34], impedencemetric [35], calorimetric [33], chemoresisters [36], field effect transistor [37], chromatographic [38] conducting polymer [39], carbon nanotubes [40] and biochemical sensors [41].

   - **Solid state gas sensor:** The principle of the solid state sensors is the change in the physical property on account of the adsorption/desorption of the gas on the sensor surface. The key property is the resistance change; this change in the resistance is converted into measurable electrical signal. The important characteristic of the gas sensor is a reversible interaction of the gas with the sensor surface. This characteristic has great interest due to its economic cost, small size, better sensor performance, possibility of real time on-line monitoring and bench production.

   - **Catalytic sensor:** Catalytic sensors are employed for combustible gas detection in the ambient atmosphere, using a certain catalyst to sustain the reactions at moderate

temperatures. The catalytic palletised surface is fabricated around the platinum coil i.e. micro heater to heat the catalyst to adequately high temperature, where the combustible gas molecules burns and release heat [42]. The compensator is composed of a reference resistance which is made up of platinum coil fixed in an alumina bead. It compensates the effects of several environment factors and obstructs oxidation of gases other than the volatile combustible gases. The catalytic sensor works on the principle is the reaction of combustible gas with the surface of the catalyst. These oxidation reactions release the heat, and change the resistance of wire due to the increase in the temperature [43].

- **Metal oxide semiconductor sensors (MOX):** The unique chemical, physical, electrical, magnetic, electronic and optical properties and capability to act as semiconductor [44] is the trademark of MOX to use them in the field of sensors. MOX semiconductor sensors are made up of nanoparticles. The sensing material presents a big surface to volume ratio, is mounted on a heater with ohmic contacts. The change in the free charge carrier concentration is observed on account of the reaction of gas molecules with the sensor surface. The sensor output is recorded in the form of the resistance change in the presence of the test gas.

5. **Sensor characteristics:** The chemical gas sensor principle is the interactions among the test gas molecules and the sensor surface. The main parameters of the nanostructured material characterization are morphology, crystal structure, particle size, porosity and electronic structure. These parameters are used to study the sensor performance. The sensor performance is measured in terms of sensitivity, selectivity, resolution, dynamic range, detection limit, response time and recovery time.

- **Sensitivity:** Sensitivity is a change in physical or chemical properties of the sensor upon injection of the test gas. Sensitivity is also known as a sensor response. It refers to the lowest concentration of gas that can be detected by the sensor.

If Ra and Rg are the sensor resistance in the presence of air and test gas respectively. The percent sensitivity (%S) is given by equation:

$$(\%\boldsymbol{S}) = (\frac{\boldsymbol{Ra-Rg}}{\boldsymbol{Ra}}) \times \mathbf{100} \qquad \text{---------- (1.6)}$$

- **Selectivity:** It is the capacity of the sensing material to respond to a specific test gas from the mixture of the gases. Selectivity of the sensor (Sij) compares sensitivity to be monitored (*Si*) to the sensitivity of the interfering stimulus (*Sj*) [45]. The ability to instantaneously differentiate and exclusively perceive a particular from the mixture of the interfering gases [46]. Sensitivity is defined as follows [45]:

$$\boldsymbol{selectivity}\ (\boldsymbol{S_{ij}}) = \frac{\boldsymbol{S_i}}{\boldsymbol{S_j}} \qquad \text{---------- (1.7)}$$

In the form of percentage as

$$\%\boldsymbol{selectivity}\ (\boldsymbol{S_{ij}}) = \frac{\boldsymbol{S_i}}{\boldsymbol{S_j}} \times \mathbf{100} \qquad \text{---------- (1.8)}$$

- **Detection time (T_{det}):** During this time the sensor output rises greater than 10% of its initial value after a test gas has been introduced on the sensor surface in a step function (Figure 6)

- **Response time (T_{res}):**During this time the sensor output attains 90% of its saturation value after a test gas has been introduced on the sensor surface in a step function

- **Recovery time (T_{res}):** During this recovery time the sensitivity descent 90% of its saturation value once the test gas is removed from the sensor surface in a step function.

- **Stability:** Stability is the sensor's ability to have constant response over a time interval.

- **Reproducibility:** Reproducibility is the measure of sensor similarity behaviour. If n number of sensors are characterised, R_k is the sensor response it can be calculated as [45]:

$$\boldsymbol{Q}(\%) = \left(\frac{\left(\frac{1}{n}\right) \sum_{k=1}^{n} \boldsymbol{R_k}}{\boldsymbol{R_{max}}} \right) \times \mathbf{100} \qquad \text{---------- (1.9)}$$

The value ranges from 0 to 100.

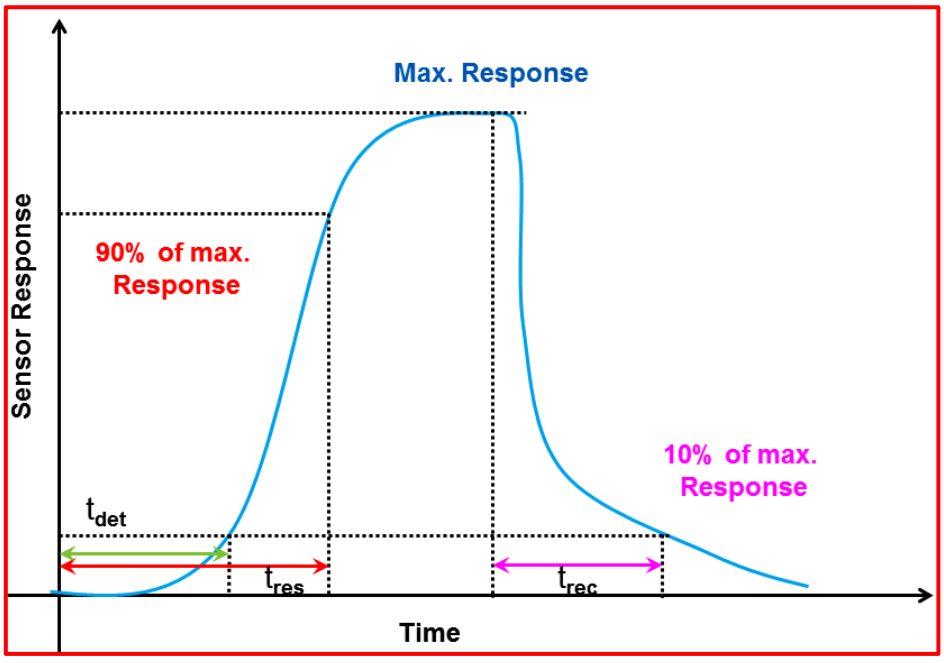

Figure 6: response, recovery and detection time.

6. Factors affecting on the performance

- **Long term effects / Baseline Drift:** Sensors operating over long time the not only baseline but also response is important factors. As these factors determine the frequency at which the sensors are to be calibrated and changed. These parameters are

defined only over long time interval. There is not any method to enhance the performance of the sensor [47].

- **Sensor surface poisoning:**The metal oxides surface may become unstable because of the poisoning phenomenon. Sulfur (as H_2S) is a potential poison in the surface poisoning. The sulphur poisoning can stop the catalytic activity on the surface of sensor. Chlorine gas is another major poison causes the Pd catalytic activity on the sensor surface to block. Therefore it is must to know about other reactive gases in the measurand environment [47].

7. Ways to improve the sensor

- **Use of catalyst:** There are several ways to boost the sensor performance. One of the ways is addition of catalyst. This is explained as below. MOX gas sensors require a catalyst to accelerate the reaction rate which can enhance the response. A catalyst is defined as a substance which can increase the reaction rate without itself getting altered. Catalysts do not increase/decrease the free energy of the chemical reaction. Catalysts decrease its activation energy. Catalysts accelerate the response speed as well as improve the specificity of gas sensors [48]. Nano-particles, with higher surface area, act as catalysts. Figure 7 illustrates the catalyst effect.

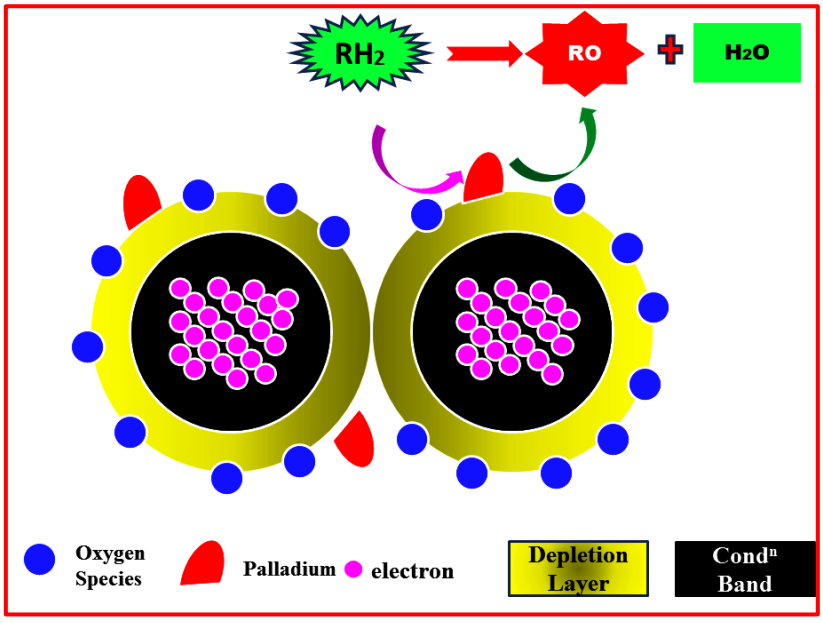

Figure 7: illustration of catalyst effect

The type of catalyst selected affects the selectivity/specificity of MOX sensor. If a specific gas in a mixture is to be detected a catalyst combination is used such that it can catalyse the oxidation reaction of the gas under study but not the oxidation of other gas in the mixture has to be selected. However, it is difficult to find ideal combinations of catalyst [49]. The extensive applicability of MOX gas sensor such as SnO_2, is associated with both the range of resistance change and to the fact that it responds to both types of gases. Minute quantities of noble metal are usually deposited on the surface of MOX a sensitizers to enhance response, specificity and to

decrease working temperature [50, 51]. The catalyst can influence gas response properties in turns affects the sensor material resistance by two different ways. One of the ways is the spill over mechanism and other is Fermi energy control.

- **Spill-over mechanism:** Spill-over mechanism is a very famous effect in heterogeneous catalysis. In spill-over mechanism additives support the redox process. Spill-over is a process in which the catalyst dissociates the gas molecule, and resulting atom can spill-over the sensor surface. Here, reactants react with pre-adsorbed oxygen species, affecting the surface resistivity.

Figure 1.8 illustrates the schematic of Spill Over mechanism. Oxygen approaches the catalyst; it causes the dissociation of oxygen [52]. To control the sensor conductance, the spilled-over species have to migrate to the inter-granular contact (Figure 9). Hence, for the operational catalyst good catalyst dispersion is necessary. The good dispersion of catalyst enables the said effect near all inter-granular contacts and hence catalysts can influence the significant inter-granular contact resistance.

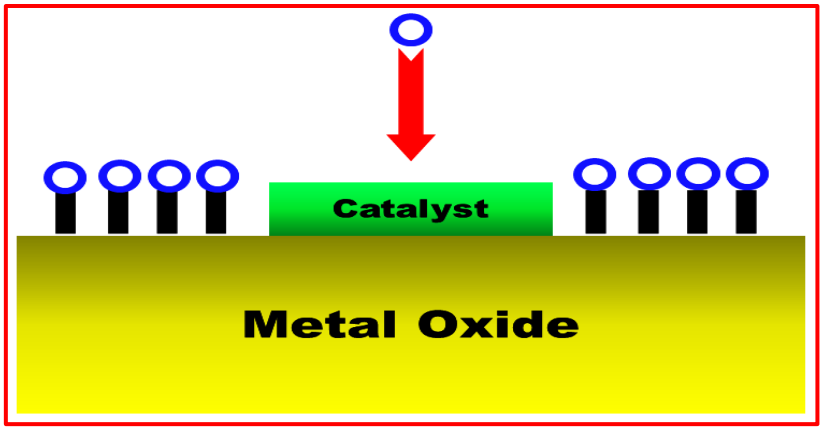

Figure 8: Schematic of spill over phenomena.

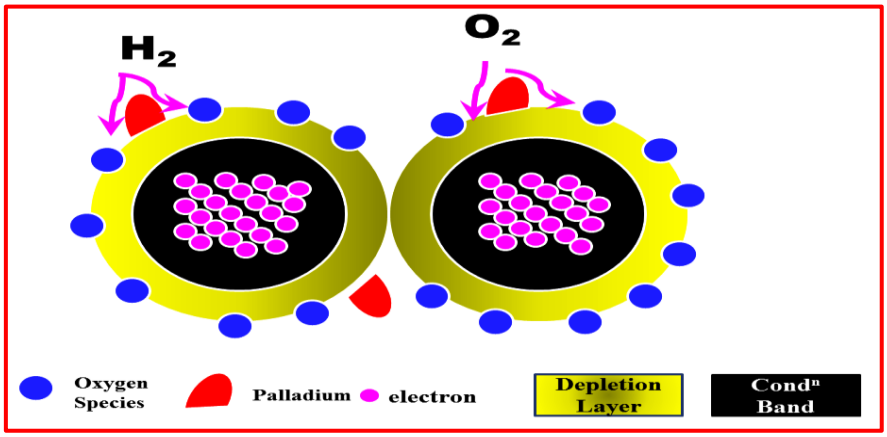

Figure 9: Illustration of Spill Over mechanisms.

The converse effect may also take place [53]. When a freshly formed nascent oxygen atom on a metal oxide surface migrates to a metal site and gets desorbed in the form of oxygen molecule. This is known as reverse spill-over effect.

- **Fermi energy control:** In the second type of interaction additives interact electronically with the MOX. The changes in the work function of the additive in the presence of a gas results in the Schottky barrier change between the metal additive and metal oxide. This process produces the change in resistivity of the sensor. The O_2 get adsorbed on the sensor surface to form O^- species by extracting the electrons from the catalyst. Consequently catalyst extracts the electrons from the supporting metal oxide semiconductor [54]. The Fermi energy control phenomenon is depicted in Figure 10.

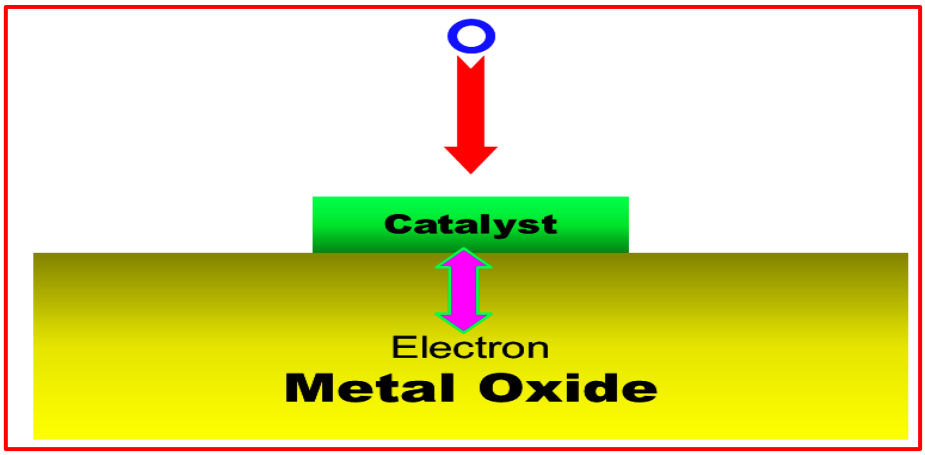

Figure 10: schematic for Fermi energy control phenomenon.

The electron depletion is governed by Fermi energy control from the metal oxide surface; however the poor catalyst distribution inhibits the effect on inter-granular contact resistance (Fig 1.10). Though some of the catalyst particles are available, only a very small surface region of the MOX surface has a surface barrier consequently, there is a less probabilities of a catalyst particle being close to the inter-granular contact to dominate surface barrier.

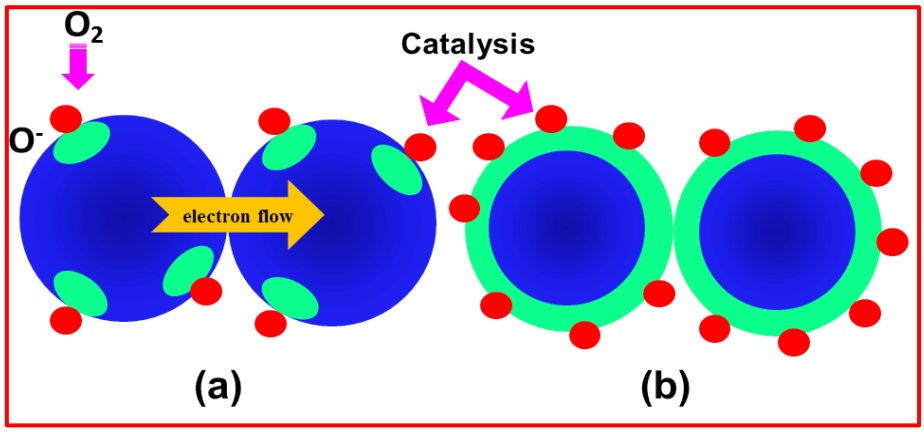

Figure 11: an adequate dispersion of the catalyst.

Figure 1 shows a good dispersion of the catalyst particles at the MOX surface and the influence of the catalyst at the inter-granular contact.

- **Grain size effects:** The microstructure of polycrystalline element is one of the essential factors affecting the gas response performance. Each crystallite of MOX has an electron depleted region. This depletion depth is up to a Debye length (L). If the crystal diameter (D) is comparable to 2L, the entire MOX crystallite gets exhausted of charge carriers. Consequently, the sensitivity towards the reducing gas changes with D. The MOX crystallites are connected with each other either by necks or grain boundary contacts. In first case electrons move through the channel penetrating through each neck. The channel aperture is diminished by the surface space charge layer. This model is associated with the grain size through the neck size. It has been observed that the neck size X is proportional to D (proportionality constant of 0.8 ± 0.1). In second case the electrons move across potential barrier. The barrier potential height varies with surrounding atmosphere. As a result the grain boundary contact is independent of the grain size. There are three cases as follows:

  - Case-I) If D>>2L, electron conduction in the element is dominated by conduction through grain boundary contacts.
  - Case-II) If D≥2L, neck control forms the primary mechanism of conductivity modulation.
  - Case-III) If D<2L, the electrical resistance of the grains controls entire sensor resistance as a result of this sensor response is controlled by grains.

Figure 1.12 and 1.13 depicts the grain size effects respectively.

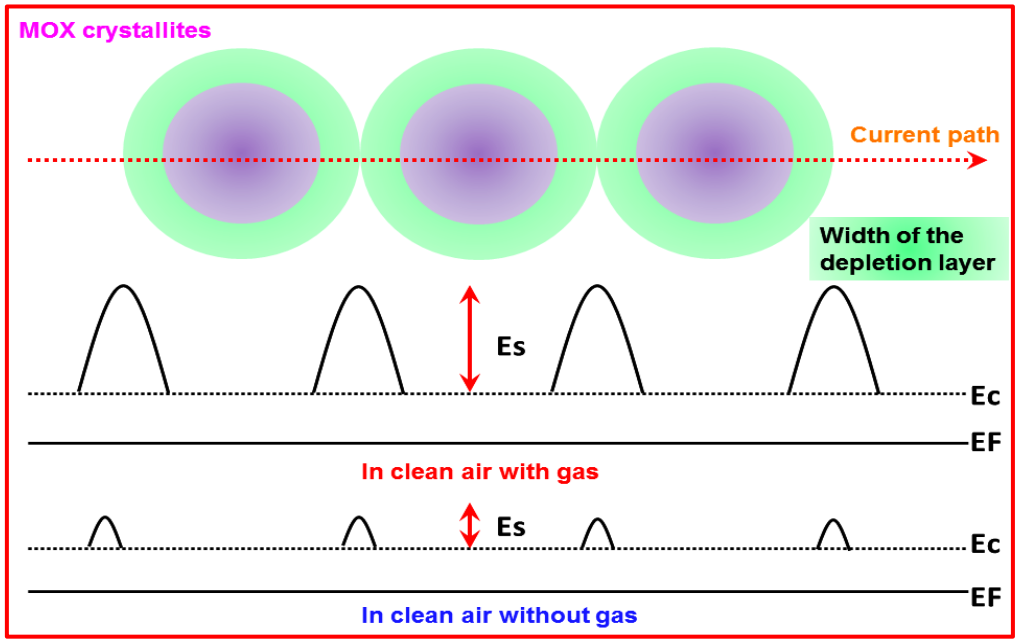

Figure 12: Crystallite size > depletion width, (incomplete depletion) and energy barrier for electron in both presence and absence of gas.

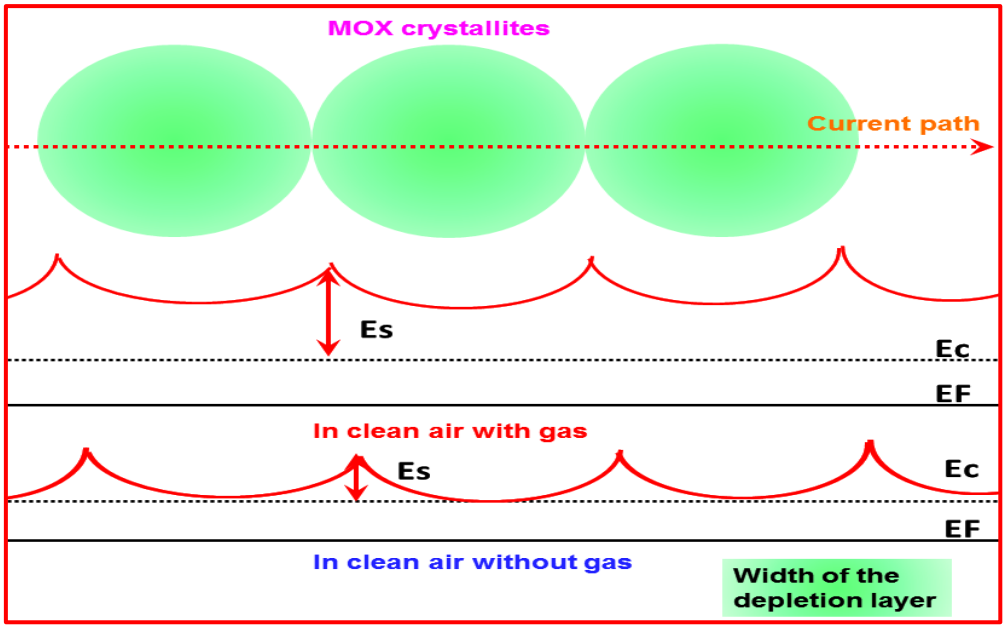

Figure 13: Crystallite size=depletion width, (complete depleted grain) and energy barrier in both presence and absence of gas

- **Thickness dependence:**Thin and thick film of MOX exhibits different transducer functions as the sensing film varies in both thickness and microstructures [55]. The gas response property of sensor is dependent intensely on the thickness of layers. When the electron depletion layer width is about the film thickness, high gas sensitivity may be expected. Therefore, gas response properties of the MOX sensor is directly affected by the depletion layer size. This effect has been as illustrated in the Figure 1.14. In general, when the depletion layer width is same as the film thickness, enhanced sensitivity can be expected.

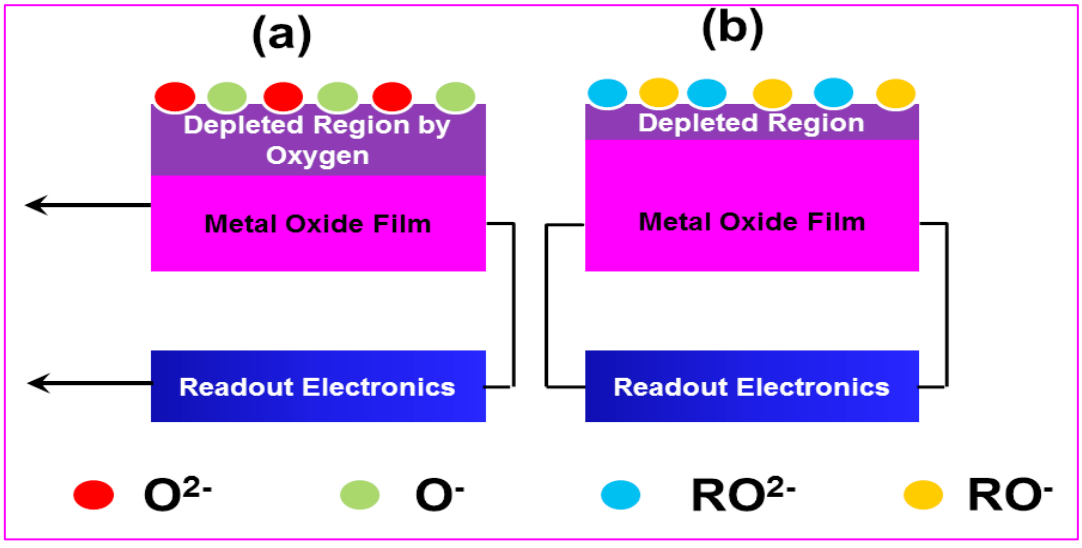

Figure 14: Sensitivity dependence on the depletion layer depth (a) Oxygen adsorption (b) Exposure to the reducing gases.

Figure 1.14(a) illustrates the depletion layer depth in the surrounding atmosphere whereas; Figure 1.14(b) illustrates the depletion layer depth reduction upon exposure to the reducing gases. While the depletion depth is approximately similar to thickness of the sensing film, the resistance becomes very high and therefore higher selectivity is expected. However, for columnar growth of film sensor behaviour is independent of film thickness [56]. The sensitive layer thickness plays a critical role towards sensor response for different gases [57]. If the film thickness is in the range of 50-300 nm it responds to the oxidizing gases and if the thickness is in the range of 15-80 μm it respond to reducing gases. However, the thick film exhibited a substantial response towards oxidizing gases at reduced operating temperatures. This behaviour can be explained with the diffusion reaction model [57].

- **Temperature modulation:** The optimum operating temperature is one of the most vital parameter of the sensor. Firstly, adsorption/desorption phenomena depends on the temperature, therefore sensors dynamic properties are influenced by the temperature variations. There are several temperature dependent reactions such as surface coverage, co-adsorption, chemical decomposition etc. As a result sensor exhibits different static properties at different temperatures. Secondly, carrier concentration, Debye length and work function etc are also influenced by the temperature. The temperature at which the sensor material is able to catalytically reduce or oxidize the target gas, instantaneously changing the electrical properties of the sensing material is called as optimum operating temperature. The reaction rate is determined by the exact reducing gas under investigation. A peak in the response curve can be observed for a given reducing agent at an optimum operating temperature: At the temperature lower than the optimum temperature the reaction rate is too slow to provide a peak in response curve, on the other hand at the temperature higher than the optimum temperature, the overall oxidation reaction takes place very quickly consequently the diffusion of reducing gas at the surface of the sensor becomes limited and hence the concentration realized by sensor approaches to zero [58]. At these temperatures, the entire test gas concentration reaching the sensor surface could get either reduced or oxidized failing the noticeable change in the resistance. Consequently the response is low again. The optimum working temperature can be determined empirically so as to provide the highest response towards the target gases. Thus, detailed understanding of the relationship among the various parameters such as sensing material, catalytic properties and response is crucial to realize the gas sensing mechanism. Therefore, an optimum temperature must be selected. For higher degrees of selectivity, sensor arrays are used for identifying the gaseous species. Such sensor array eliminates the lack of selectivity of the single MOX gas sensor. The sensor array may consist of either same sensor materials operating at different operating temperatures or the different sensors materials operating at same temperature [59-61].

- **Filters for selectivity:** Filters are used to improve the selectivity of the sensors. The filters either consume undesirable gases or allow the passage of desired gases. The use of filters is to a great extent empirical. The low porosity materials such as Carbon cloth can be used to prevent highly reactive/large gas molecules from reaching the surface of the sensor. On the other hand hydrogen molecules pass more freely through a silica surface layer. Thus Silica can be used to increase hydrogen sensitivity.

Similarly Teflon can be used for stopping H_2O reaching the sensor surface and Zirconia can be used to pass oxygen to the sensor surface [62].

8. **Gas Sensing Mechanism:** The gas sensing mechanism of MOX semiconductor gas sensors is based on the surface reactions, the charge transfer process and the transport phenomenon within the sensing layer. It takes place in the five different reversible steps as follows:
   1. Gas diffusion to the sensor surface
   2. Gas absorption at the active sites
   3. Surface reaction.
   4. Desorption of the reaction products from the active site.
   5. Diffusion of the reaction products away from the surface.

9. **Adsorption Mechanism:** It is a spontaneous process between the gas molecules and MOX surface. The free energy of this process is negative. It depends on the surface structure composition and gas molecules. It occurs in several ways which are as follows:

   Physisorption
   Hydrogen Bonding
   Chemisorption
   Ionosoption

   - **Physisorption:** It is the adsorption of gas molecules onto the MOX sensor surface, without having a change chemical and geometrical electronic structure of the gas molecule as well as the surface of the sensor. It is usually associated with dipole-dipole interaction between the gas molecule and the sensor surface. It occurs at the initial state of interaction of adsorbate with the surface. There is a weak electrostatic interaction between adsorbate and sensor surface. It can be explained by two ways as Van-der-Waals forces or dipole-dipole interaction. This is reversible process with no activation energy. The equilibrium stage is quickly attained.

     At low temperatures (<100^{o}C) it is characterised by large surface coverage θ with gas molecules and vice versa. Up to the monolayer formation the fractional surface coverage is defined by the following equation. [63].

     Therefore,

     $$\boldsymbol{\theta = \frac{N}{N_i};} \qquad \textbf{---------- (1.10)}$$

     Where, N and N_i are the number of gas molecules adsorbed per unit surface area and the total number of surface adsorption sites respectively.

     The change in the fractional coverage with time is called as rate of adsorption (dθ/dt).

     The potential of interacting particles can be described by Lennard-Jones potential (Figure1.15) [64]. It is approximated by the two particles potential (attractive and repulsive potentials). If E_{attr} is the attraction energy; d: distance

between the interacting particles and ε: depth of potential, r is the distance between the atoms in a molecule then the potential energy (E_{pot}) is given as follows:

$$\boldsymbol{E_{pot} = E_{attr} + E_{rep}\alpha\varepsilon\left[-\left(\frac{d}{r}\right)^{6} + \left(\frac{d}{r}\right)^{12}\right]} \quad \text{---------- (1.11)}$$

- **Hydrogen Bonding:** It is the electrostatic interaction in which the magnitude of interaction lies between Physisorption and chemisorption (~0.1 eV) [64]. In this bonding a covalently bonded hydrogen atom forms a second bond with another atom. The hydrogen bond typically has X-Y form where X is an atom having electronegativity greater than hydrogen and Y is any σ or π electron donor site (Lewis base). It can be symmetrical or asymmetrical, in symmetrical bond; the proton can tunnel between two equilibrium positions. On the other hand in case of asymmetrical bond the proton is more strongly bound to one atom than to another. The intermolecular force of hydrogen bonds comprises two terms. One of them is Van-der-Waals and other is covalent term. Following function (1.12) describes the he potential energy of hydrogen bond.(Fig. 1.15).

$$\boldsymbol{E_{pot} = E_{attr} + E_{rep}\alpha\varepsilon\left[-\left(\frac{d}{r}\right)^{6} + \left(\frac{d}{r}\right)^{9}\right]} \quad \text{---------- (1.12)}$$

- **Chemisorption:** It is a typical chemical reaction where the adsorbate interacts with the adsorbate through the process of the charge transfer. An interaction between adsorbate and adsorbate is much stronger than physisorption (>5 eV). It can occur in the form of atom or molecule of gas. The adsorption of molecule proceeds by the process namely dissociation of gas atom or gas molecule. It modifies the electronic structure of the adsorbate and adsorbate. The chemical bond can be formed due to the electron capture from the adsorption complex or by releasing it into the conduction band of the semiconductors. The corresponding changes in the free charge carrier concentration can be measured in terms of resistivity.

If ΔE_A is the activation barrier and ΔH_{chem} is the heat of chemisorption the net change in the chemisorption is the difference between in adsorption desorption rates (Lennard-Jones model) is given by following expression [65].

$$\frac{d\theta}{dt} = k_{ads}e^{\left(-\frac{\Delta E_A}{kT}\right)} - k_{des}\theta e^{\left(-\frac{\Delta E_A + \Delta H_{chem}}{kT}\right)}$$

The heat of chemisorption is same as the binding energy.
Therefore,

$$\frac{d\theta}{dt} = k_{ads}e^{\left(-\frac{\Delta E_A}{kT}\right)} - k_{des}\theta e^{\left(-\frac{\Delta E_A + E_{binding}}{kT}\right)}$$

The minimum energy required for the chemisorption of gas molecule is called as Activation energy. At equilibrium, adsorption rate is same as desorption rate ($d\theta/dt=0$ or $dH/dt=0$). Therefore, the coverage is given by:

$$\boldsymbol{\theta = \frac{k_{ads}}{k_{des}}e^{\left(\frac{\Delta H_{chem}}{kT}\right)}} \quad \text{---------- (1.13)}$$

- **Ionosorption:** It is a type of chemisorption. In Ionosorption the atoms/molecules are ionized by capturing an electron from the adsorbate surface. In this case adsorbate

acts as a surface state capturing the electrons from the bulk of the MOX. Ionosorption can also be named as delocalised chemisorption. Both the chemical activity and electronic and geometrical structures of the molecules are strongly influenced by the charge transfer between from molecules to surface (vice versa) [64].

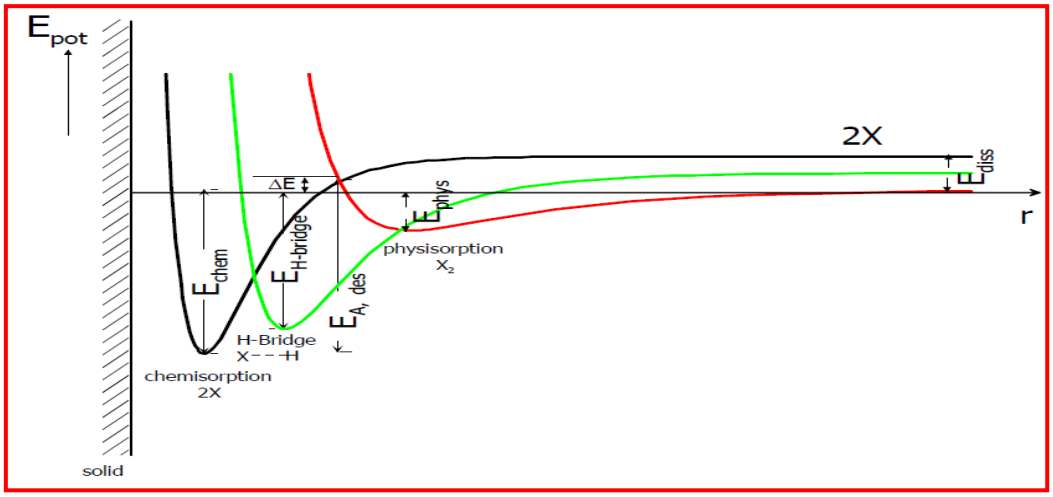

Figure 15: Potential diagrams (chemisorption, hydrogen bonding and physisorption).

The potential variations of physisorption, hydrogen bonding and chemisorption on the sensor surface are as illustrated in Figure 1.15. In case of ionosorption the adsorbate acts as a surface state, capturing charge carrier, and is held to the surface by electrostatic force of attraction. Ionosorption of oxygen in gas sensors has a prime importance and takes place in several forms viz. O_2^-, O^- and O^{2-}. Analysis of oxygen adsorption on n-type semiconductors suggests that at low temperature and high pressure of oxygen gas gets adsorbed oxygen in the usual form of O_2^-. At elevated temperatures, the O_2^- (superoxide) dissociates to the form O^- (peroxide). The peroxide form O^- is supposed to be more reactive form of oxygen. This form usually makes n-type semiconductors moderately active. The third form of oxygen is doubly charged (O^{2-}). This form of oxygen species is not in generally expected for adsorption as such high charge may cause instability.

It is well-known fact that the gas sensing mechanism of MOX semiconductors is a surface controlled process. The gas adsorption depends on both the type of test gas and the sensor material. It might not only influence the sensitivity but also response time of the sensor. Larger concentration of the test gas adsorbed enhances response due to the more favorable the reaction between the adsorbed reducing gas and oxygen species. At equilibrium at the operating temperature, oxygen species such as O^-, O^{2-}, O_2^- localize mobile electrons from MOX semiconductor (n-type) in the presence air atmosphere, resulting in a depletion layer at the surface as well as at the inter-granular regions. Afterwards, the reducing test gas reacts with the charged oxygen species destroying the process of electron localization. It can be reflected in the form of change in resistivity of the sensor material [66].

The surface and interface states of the sensing material are called intrinsic states [67, 68]. Moreover extrinsic states can be generated by test gas adsorption [67-

70]. The local electronic states result in electronic trapping processes. If the process of electronic trapping occurs in adsorbed atom or molecule is also known as ionization. Figure 1.16 describes the connected semiconductor grains and the electronic energy band at the grain boundary region. In case of n-type semiconductor the electronic interface states at the grain boundary are acceptor of type. Figure 1.16 illustrates energy bands plotted along the *x*-axis in the grain-boundary region, and electron trapping in an acceptor-type electronic interface state. Electron trapping in the interface state produces local charge at the grain boundary (density of occupied interface states N_B) which in turn, results in the electronic energy bands bending. The bending of energy band is attributed to the grain-boundary potential barrier (V_B). It determines the electron transport across the grain boundary.

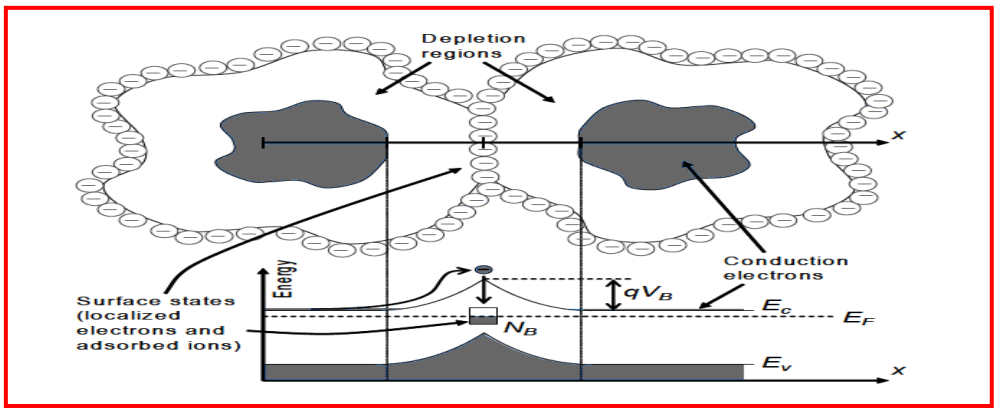

Figure 16: Schematic diagrams of two interconnected grains of n-type semiconducting material.

The effect of holes in an n-type semiconductor (wide band gap) is usually neglected and the electronic trapping takes place at the grain-boundaries. Fig. 1.17 shows the electronic energy bands in the grain-boundary region in the flat-band and in the thermodynamic equilibrium.

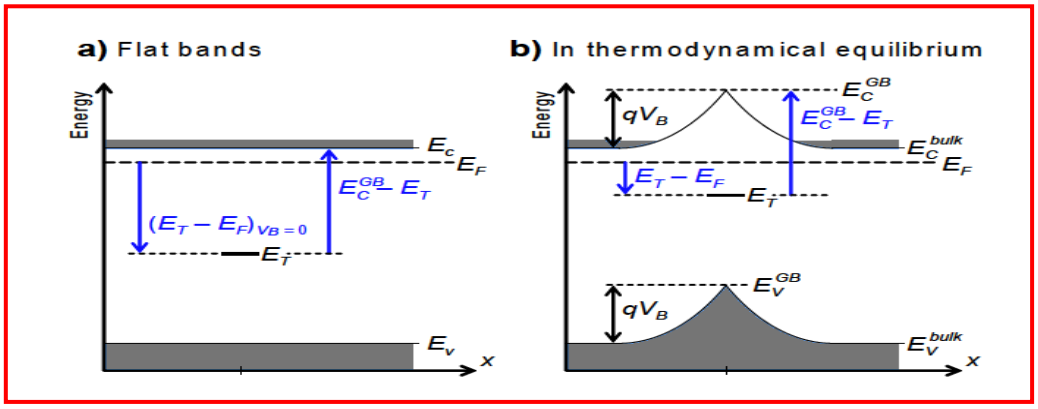

Figure 17: Schematic of electronic energy bands of n-type semiconductor at the grain-boundary region.

Electric fields cause depletion or accumulation of major charge carriers of the semiconducting material. The large depletion of major charge carriers causes the

accumulation of minority charge carriers in the region [71, 72]. This phenomenon is called as inversion. The direction of band bending in turn causes the depletion or accumulation of majority or minority charge carriers. Acceptor interface states and donor interface states in case of an n-type semiconductor causes depletion/inversion and accumulation of charge carriers respectively.

10. Types of adsorption depletion models: The process of Adsorption is generally studied with the help of the graph known as adsorption isotherm. Adsorption Isotherm is the plot of the amounts of adsorbate (x) adsorbed on the surface of adsorbent (m) versus pressure at constant temperature. There are several types of adsorption isotherms modified in different types of models, which are developed to explain the adsorption phenomenon. These are Langmuir, Braunauer-Emmett-Teller (BET), Freundlich, Wolkenstein and Kolmogorov Model.

- **Langmuir Model:** Irving Langmuir proposed that sorption rate depends on the actual concentration in the bulk and to the number of unoccupied adsorption sites. Whereas, desorption rate depends merely upon the number of sites occupied by the solute molecules. Hence the adsorption/desorption processes depends on the nature of adsorbate, the availability of adsorbate and on the temperature. The assumptions of Langmuir model are as follows:

  - Fixed numbers of adsorption/ vacant sites are always present on the solid surface.
  - Each vacant surface site is of same size and shape on the surface of the adsorbent.
  - Each vacant site will be occupied by single gaseous molecule liberating a fixed amount of heat.
  - A dynamic equilibrium is established between adsorbed molecules and the free gaseous species desorbed.
  - Adsorption is monolayer

  The Langmuir Adsorption Equation is as follows:

$$\theta = \frac{KP}{1+KP} \qquad \text{---------- (1.14)}$$

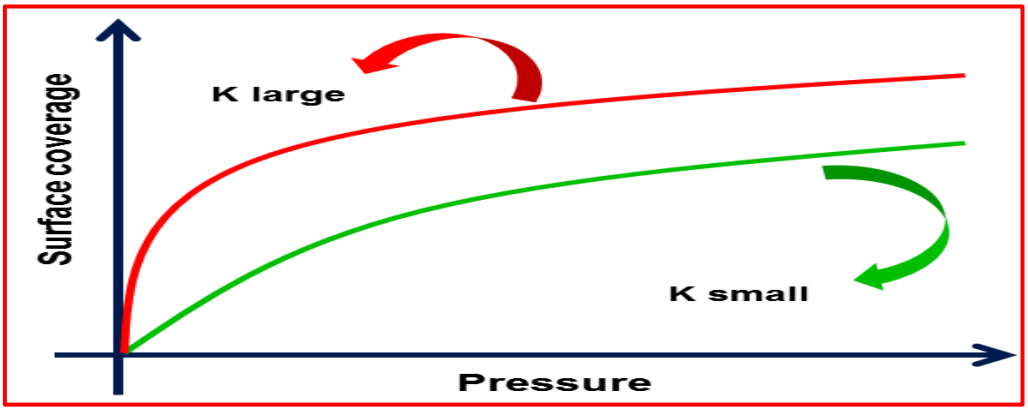

Figure 1.18 Langmuir Isotherms

Drawbacks

- It is followed only under low pressure conditions.

- It assumes that adsorption take place as monolayer but these types of process is impossible under high pressure condition.
- The assumption of homogeneous solid does not exist in all practical cases.
- Though it is assumes that molecules do not interact with each other, but weak attraction force exists even between same types of molecules.
- The adsorbed molecules are not always localized i.e. (ΔS is not 0) due to the liquefaction of gases.

Thus, it can be concluded that, Langmuir equation can be valid only under low pressure situations.

- **Braunauer, Elmer and Teller (BET) model:** As the Langmuir fails under certain conditions, Braunauer-Elmer-Teller (BET) proposed another model called as BET model which is simply the extension of Langmuir model which incorporated the multilayer adsorption. The BET model is based on the assumption as follows:

  - All the vacant surface sites are having equivalent adsorption sites;
  - Molecules of gas are adsorbed physically on all solid layers;
  - Surface layers do not interact with each other;
  - All the layers other than first layer are weakly adsorbed;
  - Langmuir theory can be valid for each layer.
  -

  If, p and p_0 are the partial pressure and the saturation pressure of gas at given temperature; V and V are the volume of the gas adsorbed at STP and volume of the gas adsorbed at STP to produce an apparent monolayer on the surface of the sample; a is a constant;
  The BET equation is given as follows:

$$\frac{p}{(p_0-p)V} = \frac{1}{aV_m} + \frac{a-1}{aV_m}\frac{p}{p_0} \qquad \text{---------- (1.15)}$$

  The BET equation is used to estimate the surface area and morphology of the sample.

- **Freundlich model:** Freundlich Model is an empirical reform of Langmuir model. It describes the multilayer adsorption as well as consequences of the sample surface heterogeneity [73]. This model considers that the inhomogeneous surface comprise of different areas. These are categorized by various inverse adsorption coefficients (b_i) *or* heats of adsorption (Qi).

  If $\frac{P}{P+b(Q)}$ is the probability of occupying an area with a given value *b(Q)* and *f(Q)* is the inverse adsorption coefficients.The degree of surface occupation is:

$$\boldsymbol{\theta = \int_{Q_{min}}^{Q_{max}} \frac{P}{P+b(Q)} f(Q)dQ = \int_{b_{min}}^{b_{max}} \frac{P}{P+b} f(b)db - 7}$$

  If α is the proportionality constant and β is the exponent then the adsorption behaviour is described by the Freundlich isotherm as [1.16]:

$$\boldsymbol{\theta = \frac{N(t)}{N} = \frac{\alpha C^{\beta}}{1+\alpha C^{\beta}}\left(1 - exp\left(\frac{t}{t_A}\right)\right)} \qquad \text{---------- (1.16)}$$

  The simplified form of Freundlich isotherm can be written as [1.17]:

$$\theta = \frac{N(t)}{N} = \alpha C^{\beta} \qquad \text{---------- (1.17)}$$

For 0<β<1

If S is the sensitivity, C is the concentration of the gas the relationship between the relative response of the sensor and concentration can be described as follows [1.18]:

$$S = \frac{\Delta R}{R}\alpha\frac{\alpha C^{\beta}}{1+\alpha C^{\beta}} \qquad \text{---------- (1.18)}$$

The expressions (1.19) and (1.20) describe the time dependence response performance S(t) during response time $S_{res}(t)$ and recovery time $S_{rec}(t)$ is as follows[1.19].

$$S_{res}(t) = A_{res}\left[1 - exp\left(-\frac{t}{t_{res}}\right)\right] \qquad \text{-------- (1.19)}$$

$$S_{rec}(t) = A_{rec}\left[1 - exp\left(-\frac{t}{t_{rec}}\right)\right] \qquad \text{-------- (1.20)}$$

However it is found that this model fails at higher concentrations [1.20].

- **Wolkenstein Model:** Wolkenstein model describes the chemisorption in terms of the electronic interactions and their effect on the absorptivity of sensor surface. Here, the localised electronic states, serves as traps for electrons or holes [77].

  The Wolkenstein adsorption isotherm is based on following assumptions:

  - There is only one gas species for adsorption.
  - Chemisorption is only source of charging.

  This adsorption process can occurs by transforming adsorbed particles from neutral state to ionized state, vice versa. The first step does not involve electronic transfer from bulk to the surface or vice versa as a result the bond is weak. The electrons of the atoms or the molecules remain located in the vicinity of the adsorbate involving the simple deformation of orbitals [78]. The electrical properties of the material do not get changed during this neutral chemisorption, but the perturbation created by the adsorbate induces surface state, E_{SS} in the band gap. Thus, the surface state acts as a trap for the electron.

  In second step occurs when an electron from the conduction band (E_C), is transferred from the semiconductor to the adsorbed species. The binding energy of the adsorbate is increased by $E_S=E_C-E_{SS}$. The process comprises the formation of a superficial negative charge and surface potential induced by chemisorption V_S (V_S <0). The surface potential V_S (V_S <0) chemisorption-induced is defined by Poisson's equation.The surface coverage θ is as follows [1.21]:

$$S_0(1-\theta)\frac{p}{\sqrt{2\pi mkT}} = N^{*}\theta^{0}v^{0}exp\left(-\frac{E_{ads}}{kT}\right) + N^{*}\theta^{-}v^{-}exp\left(-\frac{E_{ads}+E_C^b-E_{SS}}{kT}\right) \qquad -(1.21)$$

Where S_0=adsorption probability, m is the target gas molecular mass, p= the ambient gas partial pressure, k=Boltzmann constant, T=the thermodynamic temperature, θ=total coverage, θ^o=partial coverage, θ^-=partial coverage of charged adsorbate, $E_C{}^b$=conduction band edge, $v^0$and $v^-$are desorption probabilities.

For non-dissociative chemisorption the Wolkenstein adsorption isotherm is as follows:

$$\theta = \frac{\beta p}{1 + \beta p}$$

Where,

$$\beta = \frac{\beta_0 \left[1 + exp\left(\frac{E_F - E_{SS}}{kT}\right)\right]}{\left[1 + \frac{v^-}{v^0} exp\left(-\frac{E_C^S - E_F}{kT}\right)\right]}$$

and

$$\boldsymbol{\beta_0 = \frac{S_0}{N^* v^0 \sqrt{2\pi m k T}} exp\left(\frac{E_{ads}}{kT}\right)} \qquad \text{---------- } \boldsymbol{(1.22)}$$

Finally, the Wolkenstein adsorption isotherm resembles the Langmuir isotherm. In case of Langmuir isotherm the coefficient β_0 in is independent of the coverage θ. The applications of Wolkenstein model include stimulation of dynamic response of sensors to gas and modelling of noise in sensor signal.

- **Kolmogorov model:** The basic principle of Kolmogorov model is the target gas molecules interaction and surface of the sensor. Let, n be the concentration of the target gas at temperature *T* and partial pressure *p*, N_0 and N_t are the surface density of sites for adsorption and occupied sites sensor adsorbent surface respectively.Near equilibrium the generation-recombination can occur between the two reservoirs. If p_{ij} is the transition probability at time *s* from *i*-state to *j*-state at time *t*. The transition probability density is as follows:

$$\mu_{ij} = \lim_{s \to s} \frac{p_{ij}(s,t)}{t - s}$$

The transition probability density for a adsorption of gas molecules (response) and desorption of gas molecules (recovery) is given by μ_{10} and μ_{01} respectively. The characteristic time t_{res} and the transition probability density μ_{10} are related as follows:

$$\mu_{10} = \frac{1}{t_{res}}$$

Similarly, the characteristic time t_{rec} and the transition probability density μ_{01} are related as:

$$\mu_{01} = \frac{1}{t_{rec}}$$

The probability of transition $p_{ij}(t)$ is expressed as [79]:

$$\frac{dp_{ij}(t)}{dt} = \sum_{k \epsilon 1} \mu_{ik} p_{kj}(t)$$

At equilibrium, the absolute probability distributions that the surface site is free ($\prod_0$) or occupied by molecule ($\prod_{1)}$ is described as follows:

$$\sum_{k \epsilon 1} \prod_i \mu_{ik} = 0$$

Where,

$$\prod_0 = \left[1 + \frac{\mu_{01}}{\mu_{10}}\right]^{-1}$$

$$\prod_1 = \left[1 + \frac{\mu_{10}}{\mu_{01}}\right]^{-1}$$

Hence, the surface density of adsorbed molecules is given by:

$$\frac{dp_{10}}{dt} = \mu_{10}\prod_0 + \mu_{11}\prod_1$$

$$\frac{dp_{01}}{dt} = \mu_{00}\prod_0 + \mu_{01}\prod_1$$

Where, μ_{00} *and* μ_{11} are the densities of state 0 or 1, respectively.

With $\mu_{10}=C_N n$ *for adsorption,* $\mu_{01}=C_N n1$*for desrption and* C_N *as a coefficient of adsorption,*

$$\frac{dN}{dt} = \boldsymbol{adsorption(N) - desorption(N) = C_N n(N_0 - N) - C_N n_1 N} \quad \textbf{-------- (1.23)}$$

11. Recent developments nanostructured MOX gas sensors :

Sensing Materials	Morphology	Target gas	LDL	temp	Response	Response and Recovery (sec.)	Refn
Pt/SnO_2	Thin film	triethylamine (TEA)	7 ppb	200	136.2/100 ppm	3 /6	[85]
SnO_2 with Pt, Au, and Pd	nanoparticle	$C_9H_{18}O$	100 ppb	250	2/300 ppb	--	[86]
SnO_2	nanosheet	Acetone	--		10.2/1 ppm	--	[87]
SnO_2	porous flower	Acetone	--		30/20 ppm	--	[88]
SnO_2	nanowires	Cl_2	--	50	1785/5 ppm	--	[89]
ZnO	thin film	NO_2	--	450	94/200 ppm	--	[90]
ZnO	nanowires	Cl_2	--	400	3.13/5 ppm	--	[89]
WO_3	nanowires	Cl_2	--	250	2.90/5 ppm	--	[89]
WO_3		NO_2	10 ppb	200	150/500 ppb	3600/1800	[91]
In_2O_3	thin film	Cl_2		250	79.30/5ppm		[92]
In_2O_3	microtubes		0.1ppm	300	72/100 ppm	12/650	[93]
CuO-modified ZnO	thick film (nanoparticles)		--	RT	194/300 ppm		[94]
TiO_2/SnO_2	nanosheets	triethylamine	2 ppm	260	52.3/100 ppm	12/22	[95]
Ru doped ZnO	thin film	Propane		300	890/300 ppm		[89]
Ni/SnO_2	xerogels	H_2S	--	275	11.5/275	15	[96]
Al/SnO_2	xerogels	formaldehyde	--	300	15/100	7/16	[97]
CNT	nanotubes	NO2	0.2ppb	25	150/1ppb	120	[98]

Several research works has been published on the Web of Science [84]. Which include several materials such as SnO_2, ZnO, TiO_2, WO_3, In_2O_3, Fe_2O_3 etc. SnO_2 has attracted a great deal of interest among several sensing materials. Table 1 shows the recent development of various sensing materials, morphology, target gas used, lower detection limit (LDL), operating temperature, response, response and recovery times.

Several research works has been published on the Web of Science [84]. Which include several materials such as SnO_2, ZnO, TiO_2, WO_3, In_2O_3, Fe_2O_3 etc. SnO_2 has attracted a great deal of interest among several sensing materials. Table 1 shows the recent development of various sensing materials, morphology, target gas used, lower detection limit (LDL), operating temperature, response, response and recovery times.

REFERENCES

[1] Merriam's-Webster's Collegiate Dictionary, An Encyclopedia Britannia Company, 11th edn, 2008.
[2] S. M. Sze, Semiconductor Sensors, John Wiley & Sons, Inc, New York U.S.A., 1994.
[3] I.R. Sinclair, Sensors and transducers Newnes, Oxford, UK, 2001.
[4] P. Sazama, J. Dedeek, Mater. Lett. 62 (2008) 4239-4241.
[5] K.Lee, J.H. Kwon, S.L. Moon, W.S. Cho, B. K. Ju, Y. H. Lee, Mater. Lett. 61 (2007) 3201-3204.
[6] R.G. Deshmukh, S.S. Badadhe, M.V. Vaishampayan, I.S. Mulla, Mater. Lett. 62 (2008) 4328-4331.
[7] J.Janata, M. Josowicz, D.M. DeVaney, Anal. Chem. 66 (1994) 207-228.
[8] C. O. Park, S. A. Akbar, J. Mater. Sci. 38, (2003) 4611-4637.
[9] H. Meixner, J. Gerblinger, U. Lampe, M. Fleischer, Sens. Actuators B 23 (1995) 119-125.
[10] T. Takeuchi, Sens. Actuators B, 14 (1988) 109-124.
[11] J.T. Woetsman, E.M. Logothetis, Controlling Automotive Emissions, The Industrial Physicist, Ed. American Institute of Physics (1995) 20-24.
[12] S.B. Patil, P.P. Patil, M.A. More, Sens. Actuators B 125 (2007) 126–130.
[13] N. Barsan, D. Koziej, U. Weimar, Sens. Actuators B 121 (2007) 18–35. Vomiero, S. Bianchi, E. Comini, G. Faglia, M. Ferroni, G. Sberveglieri, Cryst. Growth Design 7 (2007) 2500–2504.
[14] S. Chakraborty, D. Banerjee, I. Ray, A. Sen, Curr. Sci. 94 (2008) 237–242.
[15] P. Sahay, J. Mater. Sci. 40 (2005) 4383–4385.
[16] L. Wang, A. Teleki, S. Pratsinis, P. Gouma, Chem. Mater. 20 (2008) 4794–4796. Teleki, S.E. Pratsinis, K. Kalyanasundaram, P.I. Gouma, Sens. Actuators B Chem. 119 (2006) 683–690.
[17] P.A. Murade, V.S. Sangawar, G.N. Chaudhari, V.D. Kapse, A.U. Bajpeyee, Curr. Appl. Phys. 11 (2011) 451–456. Srivastava, Rashmi, K. Jain, Mater. Chem. Phys. 105 (2007) 385-390.
[18] K. Jain, R.P. Pant, S.T. Lakshmikumar, Sens. Actuators B 113 (2006) 823-829.
[19] V. Kumar, S. K. Srivastava, K. Jain, Sens. Transducers 101 (2009) 60-68.
[20] F. Pourfayaz, A. Khodadadi, Y. Mortazavi, S.S. Mohajerzadeh, Sens. Actuators B 108 (2005) 172-176.
[21] V. Kuma, S. Sen, K.P. Muthe, N.K. Gaur, S.K. Gupta, J.V. Yakhmi, Sens. Actuators B 138 (2009) 587-590.
[22] S. Habibzadeh, A.A. Khodadadi, Y. Mortazavi, Sens. Actuators B 144 (2010) 131–138.
[23] W. Gopel, W.J. Hesse, J.N. Zemel, Sensors (1989)3-4.
[24] S. M. Sze, Semiconductor Sensors, John Wiley & Sons, Inc, New York U.S.A., 1994.
[25] H. Windischmann, P. Mark, J. electrochem. Society, 126 (1979) 627-633.
[26] T. G. Nenov and S. P. Yordanov, Ceramic Sensors: Technology and Applications, Technomic Pub. Lancaster 1996.
[27] H. Patel, The Electronic Nose: Ortificial Olfaction Tech., (2013) 143-180.
[28] E. I. Iwuoha, A. Al-Ahmed, M. Sekota, T. Waryo, P. Baker, Encyclopedia of Supramolecular Chemistry, Taylor and Francis, (2004) 1-18.
[29] F. Winquist, Microchima Acta, 163 (2008) 3-10.
[30] E.J. Calvo, M. Otero Springer Verlag Berlin Heidelberg (2008) 241-257.
[31] J.I. Janata, Prin. Chem. Sensors, (2009) 119-199.
[32] S. Achmann, G. Hagen, J. Kita, I. Malkowsky, C. Kiener, R. Moos, Sensors, 9 (3), (2009) 1574-1589.

[33] V.L. Kopparthy, S.M. Tangutooru, G.G. Nestorova, E.J. Guilbeau, Sens Actuators B Chem, 166-167, (2012), 608-615.
[34] D. Liu, M. Liu, G. Liu, S. Zhang, Y. Wu, X. Zhang, Analytical Chemistry, 82(1) (2009), 66-68.
[35] P. Grundler, Chemical Sensors: An Introduction for Scientists and Engineers: Springer Berlin Heidelberge, 2007.
[36] B. Adhikari, S. Mujumdar, Progress in Polymer Science, 29(7), (2004), 699-766.
[37] L. Gomez De Arco, Doctoral Dissertation, University of Southern California, U.S.A., 2010.
[38] J. Anzai, Encyclopedia of Supramolecular Chemistry. Taylor and Francis, (2004) 115-119.
[39] T. Artursson, P. Spangenus, M. Holmbege, Analytica Chimica Acta, 452(2), (2012), 255-264.
[40] S.D. Kolev, M. Adam, I. Barsony, A. van den Berg, C. Cobianu, S. Kulinyi, Michroelectronics Journal, 29(4-5), (1998), 235-239.M. Gaskov, M.N. Rumyantseva, Rassian J. Appl. Chem., 74(3), (2001), 440-444. Gurlo, N, Barsan, U. Weimar, Metal Oxides: Chemistry and Application. CRC press, (2005) 683-738.
[41] M.E. Franke, T.J. Koplin, U. Simon, 2006, "Metal and Metal Oxide Nanoparticles in Chemoresistors: Does the Nanoscale Matter?" Small, 2(1), 36-50.
[42] D.E.Williams,P.T Mosely, J. mater. Chem. 1 (1991) 809-814.
[43] J. Wollenstein, Sens Actuators B Chem. 70 (2000) 196-202.
[44] D. S. Vlachos, C. A. Papadopoulos and J. N. Avaritsiotis, Appl. Phys. Lett., 69 5 (1996) 650-652.
[45] P. Montmeat, Sens Actuators B Chem, 84 (2002) 148-159.
[46] J. Zhang, K. Colbow, Sens Actuators B Chem., 40 (1997) 47-52.
[47] U. Weimar, W. Goepel, Sens Actuators B Chem 26-27 (1995) 13-18.
[48] http://ceiba.cc.ntu.edu.tw/catalysis/course/Chap6.pdf
[49] R.K. Srivastava, Sens Actuators B Chem. 21 (1994) 213-218.
[50] F. Hossein-Babaei, M. Orvatinia, Sens Actuators B Chem. 89 (2003) 256-261.
[51] Th. Baker, Sens Actuators B Chem. 77 (2001) 55-61. Xu, Sens Actuators B Chem. 3 (1991) 147-155.
[52] S. Roy Morrison, Sens Actuators B Chem. 12 (1987) 425-440.
[53] E. Llobet, IEEE Sensors Journal, 1 (2001) 3 207-213.
A. Hagleitner, Nature, 414, (2001) 293-296.
[54] J.W. Lim, Sens Actuators B Chem 77 (2000) 139-144.
[55] S. M. Sze, Semiconductor Sensors, John Wiley & Sons, Inc, New York U.S.A., 1994.
[56] P. Reichel, Doctoral Dissertation, University of Tubingen, Tubingen (2005).
[57] S. Harbeck, Doctoral Dissertation, University of Tubingen, Tubingen (2005).
[58] M. Batzill, Sensors, 6(10) 2006 1345-1366.
[59] J. Jose, A. Khadar, Nanostruct. Mater. 11 (1999) 1091-1099.
[60] J. Ding, T.J. McAvoy, R.E. Cavicchi, S. Semancik, Sens. Actuators B 77 (2001) 597-613.
[61] J.W. Orton, M.J. Powell, Reports on Progress in Physics, 43 (1980) 1263-1308.
[62] F.F. Volkenshtein, The electronic Theory of Catalysis on Semiconductors, Pergamon Press Ltd., New York, U.S.A., 1963.
[63] T. Wolkenstein, Electronic Processes on Semiconductor Surfaces during Chemisorption, Plenum Publishing Corporation, New York, U.S.A., 1991. Many, Y. Goldstein, N. B. Grover. Semiconductor Surfaces. North-Holland Publishing Company, Amsterdam, The Netherlands, 1965.
[64] H. Luth. Solid Surfaces and Interfaces of Solids, Springer, Berlin, Germany, 4th edition, 2001.
[65] M. Gautam, A.H. Jayatissa, J. Appl. Phys., 111 (9) (2012) 094317-9.
[66] H. Hu, M. Trejo, M.E. Nicho, J.M. Saniger, A. Garcia-Valenzuela, Sens Actuators B Chem, 82(1), (2002) 14-23.
[67] J.L. Johnson, A. Behnam, Y. An, S.J Pearton, A. Ural, J. of Applied Physics, 109(12) (2011) 124301-7.
[68] S.P. Arnold, S.M. Prokes, F.K. Perkins, M.E. Zaghloul, Applied Physics Letters, 95(10), (2009) 1-3.
[69] H. Geistlinger, Sens Actuators B Chem, 119(1) (1993) 47-60.

[70] J. Guerin, K. Aguir, M. Bendahan, Sens Actuators B Chem 17(1) (2006) 327-334.
[71] P. Sedlak, J. Majzner, M. Vrnata, P. Fitl, D. Kopecky, F. Vyslouzil, P.H. Handel, Sens Actuators B Chem, 166-167, (2012) 264-268.
[72] N. Yamazoe, K. Shimanoe, 1 - Fundamentals of semiconductor gas sensors, in: R. Jaaniso, O.K. Tan (Eds.), Semiconductor Gas Sensors, Woodhead Publishing, 2013, pp. 3–34.
[73] J. Watson, The Tin Oxide Gas Sensor and Its Applications, in: Sensors and Actuators, 5, 1984, pp. 29–42.
[74] M. Madou, S.R. Morrison, Chemical Sensing with Solid State Devices, Academic Press, Boston, 1989.
[75] G. Korotcenkov, Chemical Sensors: Fundamentals of Sensing Materials, Momentum Press, New Jersey, 2011.
[76] Yoshitake MasudaRecent advances in SnO2 nanostructure based gas sensors, Sensors & Actuators: B. Chemical 364 (2022) 131876
[77] Y. Xu, W. Zheng, X. Liu, L. Zhang, L. Zheng, C. Yang, et al., Platinum single atoms on tin oxide ultrathin films for extremely sensitive gas detection, Mater. Horiz. 7 (2020) 1519–1527.
[78] Y. Masuda, K. Kato, M. Kida, J. Otsuka, Selective nonanal molecular recognition with SnO2 nanosheets for lung cancer sensor, Int J. Appl. Ceram. Technol. 16 (2019) 1807–1811.
[79] K. Kim, Pg Choi, T. Itoh, Y. Masuda, Catalyst-free highly sensitive SnO2 nanosheet gas sensors for parts per billion-level detection of acetone, ACS Appl. Mater. Interfaces 12 (2020) 51637–51644.
[80] L. Cheng, S.Y. Ma, T.T. Wang, J. Luo, Synthesis and enhanced acetone sensing properties of 3D porous flower-like SnO2 nanostructures, Mater. Lett. 143 (2015) 84.
[81] R. Lontio Fomekong, B. Saruhan, Influence of humidity on NO2-Sensing and Selectivity of Spray-CVD Grown ZnO thin film above 400 ◦C, Chemosensors 7 (2019) 42.
[82] T. Van Dang, N. Duc Hoa, N. Van Duy, N. Van Hieu, Chlorine gas sensing performance of on-chip grown zno, wo3, and sno2 nanowire sensors, ACS Appl. Mater. Interfaces 8 (2016) 4828–4837.
[83] L. Parellada-Monreal, et al., WO3 processed by direct laser interference patterning for NO2 detection, Sens Actuators B 305 (2020).
[84] K. Yuan, C.-Y. Wang, L.-Y. Zhu, Q. Cao, J.-H. Yang, X.-X. Li, et al., Fabrication of a micro-electromechanical system-based acetone gas sensor using CeO2 nanodot- decorated WO3 nanowires, ACS Appl. Mater. Interfaces 12 (2020) 14095–14104.
[85] W. Yang, L. Feng, S. He, L. Liu, S. Liu, Density gradient strategy for preparation of broken In2O3 microtubes with remarkably selective detection of triethylamine vapor, ACS Appl. Mater. Interfaces 10 (2018) 27131–27140.
[86] H. Zhang, Z. Jin, M.D. Xu, Y. Zhang, J. Huang, H. Cheng, et al., Enhanced isopropanol sensing performance of the CdS nanoparticle decorated ZnO Porous nanosheets-based gas sensors, IEEE Sens. J. 21 (2021) 13041–13047.
[87] H. Xu, J. Ju, W. Li, J. Zhang, J. Wang, B. Cao, Superior triethylamine-sensing properties based on TiO2/SnO2 n–n heterojunction nanosheets directly grown on ceramic tubes, Sens. Actuators B: Chem. 228 (2016) 634–642.
[88] NL Myadam, DY Nadargi, JD Nadargi, VR Kudkyal, FI Shaikh, IS Mulla, SS Suryavanshi, MG Chaskar Ni/SnO2 xerogels via epoxide chemistry: Potential candidate for H2S gas sensing application Journal of Porous Materials volume 28, pages239–248 (2021)
[89] Nagesh L. Myadama,b, Digambar Y. Nadargic, Jyoti D. Gurav Nadargid, Faiyyaj I. Shaikhe, Sharad S. Suryavanshic,∗, Manohar G. Chaskara, A facile approach of developing Al/SnO2 xerogels via epoxide assisted gelation: A highly versatile route for formaldehyde gas sensors Inorganic Chemistry Communications 116 (2020) 107901.
[90] P. Qi, O. Vermesh, M. Grecu, A. Javey, Q. Wang, H. Dai, et al., Toward large arrays of multiplex functionalized carbon nanotube sensors for highly sensitive and selective molecular detection, Nano Lett. 3 (2003) 347–351.

